

# Methods of Improving ABAQUS/Standard Predictions for Problems Involving Sliding Contact

Ted Diehl  
Senior Engineer  
Eastman Kodak Company  
Rochester, NY 14652-4391

ABAQUS Users' Conference Proceedings  
Paris, France  
May 31 - June 2, 1995

## Abstract

Methods of improving solution accuracy in sliding contact problems, with and without friction, are discussed. The analysis concentrates on the problem of a circular, rigid body in sliding contact with a flexible beam. Solution noise that is commonly observed when using an IRS contact algorithm is eliminated by using slide line elements such that the rigid body is discretized and defined as the "slave" surface. For problems with friction, the current ABAQUS logic in the MATFRU subroutine is shown to frequently omit frictional effects in sliding contact problems. A simple modification to this logic allows for the continuous inclusion of frictional forces which significantly improves solution accuracy.

## 1.0 Introduction

Analysis of contact is commonly performed with ABAQUS/Standard. For simplicity, we study two cases where a circular, rigid body is in sliding contact with a flexible beam. Figure 1 depicts schematics of the two examples. These problems are designed to model fundamental contact behaviors that are commonly seen when modelling snap-fit components, latches, and cam-activated switches. Although these problems look trivial, we will see that selecting the appropriate contact logic is very important to obtaining smooth and accurate results. *Furthermore, these problems will demonstrate that the current ABAQUS implementation of friction frequently omits frictional loads for many sliding contact problems of this type.*

## 2.0 Evaluation of First Test Problem

Figure 2 depicts three finite element models used to model the first example problem. Contact of the rigid circle with the flexible beam is modelled by two methods: (1) a \*RIGID SURFACE with IRS interface elements and (2) a \*SLIDE LINE with ISL elements. The first two models shown (IRS methods) use a modelling approach that most

analysts would likely choose; the *slave* nodes reside on the flexible beam and the *master* surface is defined by the rigid circle. The third model (ISL method) switches which surface is master and which is slave; the circle is discretized and defined with slave nodes while the segments along the flexible beam elements define the master surface. Listings for these three models are supplied at the end of this paper.<sup>1</sup> For all three models, the \*SURFACE CONTACT, SOFTENED option is used. For the ISL method, the use of softened contact is required to avoid the possibility of *numerical solver problems* caused by an overconstraint condition during contact. If softened contact is not used with the ISL method, then anytime three or more slave nodes are determined to be in an overclosed state along a single *linear* segment of the \*SLIDE LINE, an overconstraint condition will occur. This is because the MPC requires the three slave nodes to remain in a *circle* and the \*SLIDE LINE requires the overclosed nodes to be constrained to the straight line. Softened contact adds a spring into the constraint which allows the proper contact condition to be computed smoothly. The use of softened contact with the IRS method is not required but does help smooth out the solution and increase convergence speed, especially when friction is considered.

Figure 3 presents the theoretical solutions, with and without friction, of the vertical force  $F_y$  as a function of the vertical displacement  $\delta y$  (see the Appendix for theoretical derivation). Figure 4 compares the results of the three finite element models, without friction, to the theoretical baseline. All FE solutions utilized 20 equally spaced time increments. The results demonstrate that the ISL method is much more accurate than the IRS method (comparing similar mesh density for the flexible beam). Noise in the IRS method is only reduced by using a fine mesh (which is inefficient and overkill from a beam-bending viewpoint). The schematics in Figure 5 further demonstrate why the ISL method produces the best results for this class of problem.

Figure 6a compares the same three models for a coefficient of friction,  $\mu = 0.3$ . For these models the *current* ABAQUS implementation logic for friction was used with the penalty method. Currently in ABAQUS/Standard, frictional effects on a slave node are neglected for the increment during which contact for that node is first established, during any increment in which contact for that node is re-established, and during any increment in which contact for that node is lost.<sup>2</sup> The result of this implementation is that frictional loads in the IRS models (for this example problem) are ignored for almost every solution increment because at each new time increment the rigid circle is in contact with a different slave node.<sup>3</sup> Fortunately, the ISL method (for this example problem) performs quite well and includes all frictional loads for every increment but one. Since the point of contact on the rigid circle is in nearly the same spot (same slave node) for most of the solution, frictional forces are included. During the one increment that part of the frictional load is omitted (noted on Figure 6a), a new slave node came into contact (no friction included) while the previous slave node remained in contact (friction included). Figure 6b compares the same

---

1. The IRS method with a fine mesh is not listed. This deck is simply made from the IRS method with a coarse mesh by increasing the number of nodes on the flexible beam from 25 to 100.

2. According to HKS, this logic was originally chosen to avoid convergence and infinite loop problems for the general class of frictional contact problems, in particular, problems that have to deal with stick/slip conditions.

3. With the coarse IRS model the slave nodes are spaced far enough apart that for a few time increments the same slave node may be in contact with the rigid surface for two successive increments. In this case friction is included for that slave node only.

three models with a *modified* friction logic. As seen in the plots, significant improvement in solution accuracy has been achieved. In this modified logic, frictional effects are included whenever a node is in contact. The modified “calling” logic is included by a simple change to the *if-then* logic of subroutine MATFRU. This subroutine controls when the user subroutine FRIC is called.<sup>1</sup> The FE solutions plotted in Figure 6b used a Lagrange friction algorithm and there were no difficulties with infinite loops nor convergence. Solution with a penalty friction algorithm gave equally good results and no difficulties with infinite loops or convergence.

### 3.0 Evaluation of Second Test Problem

The first test problem demonstrated the advantage of using the ISL method to model sliding contact problems with and without friction. This second test problem (Figure 1b) further demonstrates the need for the modified friction logic. Figure 7 depicts the finite element model used in this example and Figure 8 shows the results with the *current* ABAQUS friction logic and the *modified* friction logic. All FE results are computed with 20 equally sized increments and each data point is denoted with a symbol. Figure 8a clearly shows the deficiency in the current friction implementation; because the rigid cam is rotated, new slave nodes repeatedly come into contact with the master surface at each new increment and frictional forces are frequently omitted. Figure 8b demonstrates that the modified implementation yields a very accurate solution.

As with the previous test case, no convergence problems were found with the modified algorithm. It is further noted that using the current ABAQUS logic and attempting to control the time increment size such that nodes stay in contact over multiple time increments (to include frictional effects) is not practical because it would require unreasonably small time increments for this class of problems. Also, adjusting the softened contact parameters such that nodes stay in contact over multiple time increments is not generally acceptable because it places a tedious burden on the user and often cannot be done. Finally, the use of UNSYMM had little influence on solution speed.

### 4.0 Conclusions

Analysis of sliding contact such as commonly found with snap-fit parts, latches, and cam activated switches must be done with care. For the two examples evaluated here, the ISL contact method has been shown to yield solutions that are less noisy and more accurate than those computed using the IRS contact method. *For cases with sliding friction, the current ABAQUS logic often omits frictional effects entirely.* A simple modification of the friction “calling” logic in the MATFRU subroutine corrects this problem and produces very accurate results without any degradation in convergence speed or difficulties with infinite loops, even when using a Lagrange friction approach. In general, whenever slave nodes are also constrained with rigid MPCs, the \*SURFACE CONTACT, SOFTENED option should

---

1. Subroutine MATFRU is not usually available to the user. HKS (Nagtegaal, 1993) provided this author access to the subroutine in order to change an “if-then” statement. To implement the modified friction logic of MATFRU, a user-defined FRIC subroutine was required. The FRIC subroutine used here was based on the FRIC subroutines described by Ang (1993, 1994).

be used to avoid any overconstraint conditions. Also, using softened contact with frictional sliding problems, modelled with IRS or ISL methods, usually increases convergence speed.

## Acknowledgments

Thanks to Joop Nagtegaal, George Ang, and Debbie Burton of HKS for their assistance.

## References

Ang, G. "Lagrange Implementation of Coulomb Friction Using User Subroutine FRIC," HKS Technical Note, April 5, 1994.

Ang, G. "Implementation of Coulomb Friction in User Subroutine FRIC Using the Penalty Method," HKS Technical Note, April 8, 1993.

Nagtegaal, J., Personal communication, 1993.

## Appendix: Theoretical Solutions to First and Second Example Problems

First we develop a theoretical solution for the example depicted in Figure 1a. The following equations are based on linear, small-deflection, Euler beam theory. The equations for the deflection  $u_\eta$  and slope  $\theta$  of a cantilevered beam with a point load  $F$  at  $\xi = \xi_L$ , are

$$u_\eta = \frac{-F\xi_L^3}{3EI}, \quad \theta = \frac{-F\xi_L^2}{2EI} \quad \rightarrow \quad u_\eta = \frac{2}{3}\xi_L\theta. \quad (1)$$

The point load  $F$  is caused by contact with the rigid cylinder which is defined in 2-D by the equation of a circle

$$(\xi - \xi_c)^2 + (\eta - \eta_c)^2 = r^2. \quad (2)$$

The above equation can be solved for  $\eta$  as

$$\eta = \eta_c - \sqrt{r^2 - (\xi - \xi_c)^2} \quad (3)$$

where we have chosen the portion of the circle that is closest to the beam. The slope of the circle is computed as

$$\frac{d\eta}{d\xi} = \frac{(\xi - \xi_c)}{\sqrt{r^2 - (\xi - \xi_c)^2}}. \quad (4)$$

As depicted in Figure 1a the motion of the rigid circle is constrained to move only in the Y-direction. The rigid circle's center coordinates in the XY coordinate system are mapped to the  $\xi\eta$  coordinate system as

$$\begin{aligned}\xi_c &= Y_c \cos(\alpha) - X_o \sin(\alpha) \\ \eta_c &= Y_c \sin(\alpha) + X_o \cos(\alpha) .\end{aligned}\quad (5)$$

During contact the circle touches the flexible beam at one point ( $\xi = \xi_L$ ,  $\eta = u_\eta$ ) and the slope of the beam at this contact point is equal to the slope of the circle. Combining Equations 1, 3, and 4 yields

$$\eta_c - \sqrt{r^2 - (\xi_L - \xi_c)^2} = \frac{2}{3} \xi_L \frac{(\xi_L - \xi_c)}{\sqrt{r^2 - (\xi_L - \xi_c)^2}} \quad (6)$$

where the only unknown is the contact length  $\xi_L$ . Once this is computed (numerically), the beam deflection  $u_\eta$  and the contact load  $F$  can be computed as

$$u_\eta = \eta_c - \sqrt{r^2 - (\xi_L - \xi_c)^2}, \quad F = \frac{-3EIu_\eta}{\xi_L^3} . \quad (7)$$

We see from Figure 1a that the contact force  $F$  acts normal to the circle (or equivalently, it rotates to stay normal with the beam in the deformed state).<sup>1</sup> The force that must be applied to the rigid circle in the Y-direction when it is in contact the flexible beam is derived from  $F$  as

$$F_y = -F \left( \sin(\alpha - \theta) + \mu \cos(\alpha - \theta) \right) \quad (8)$$

where  $\mu$  is the coefficient of friction.<sup>2</sup>

The second example problem (Figure 1b) is similar to the first example problem (Figure 1a). From geometry we have

$$R = \sqrt{(\xi_c - \xi_R)^2 + (\eta_c - \eta_R)^2}, \quad \sin(\phi) = \frac{\xi_c - \xi_R}{R} \quad (9)$$

where  $R$  and  $\phi$  are obtained using values of  $\xi_c$  and  $\eta_c$  in the undeformed (initial) state. Then for any rotation of  $\phi$ , we can find the current values of  $\xi_c$  and  $\eta_c$  by

$$\begin{aligned}\xi_c &= R \sin(\phi) + \xi_R \\ \eta_c &= -R \cos(\phi) + \eta_R .\end{aligned}\quad (10)$$

Utilizing the analysis of the first example problem leads to the drive moment  $M_z$  defined as

$$M_z = -F_x(\xi_L - \xi_R) + F_y(-u_\eta + \eta_R) \quad (11)$$

where

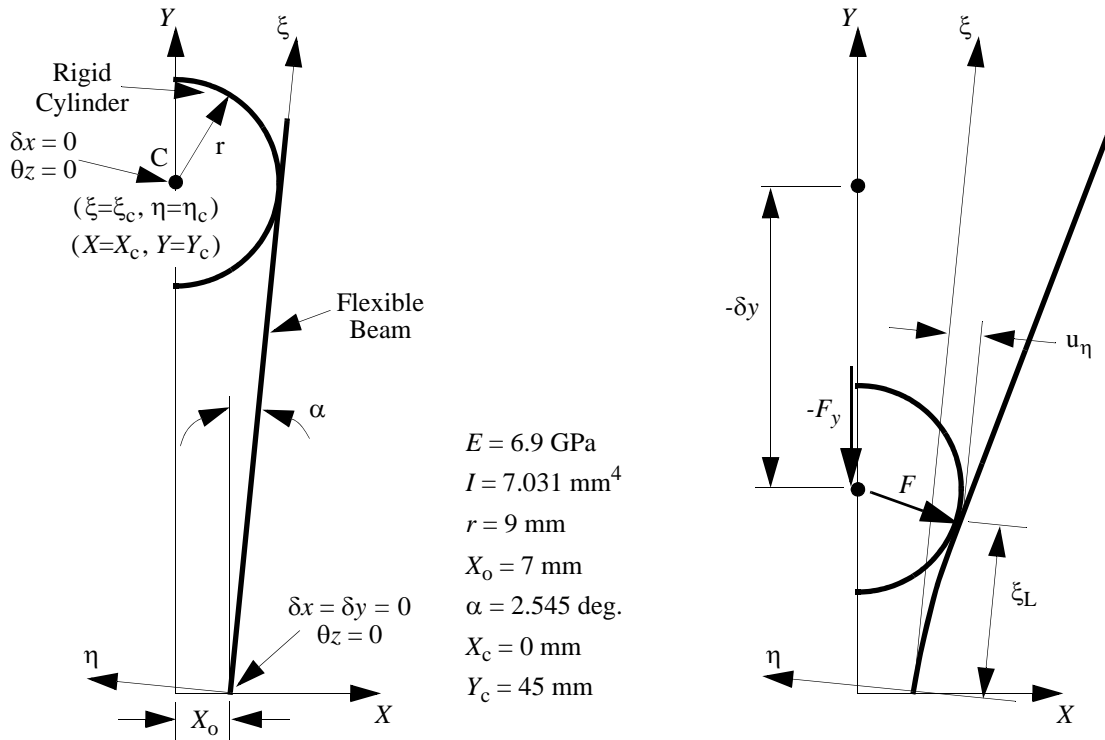
---

1. It might appear that this assertion is inconsistent with the linear beam theory used in the equation derivations. Because the beam displacements  $u_\eta$  are small, it can be shown by superposition of the vector components of the “rotated” contact force  $F$  that the vector component which acts in the  $\xi$ -direction of the beam will cause negligible beam deflection. Hence, the use of linear beam theory is valid.

2. In Equation 8,  $\theta$  is subtracted from  $\alpha$  because  $\theta$  will be a negative quantity.

$$\begin{aligned} F_x &= F (\cos(-\theta) - \mu \sin(-\theta)) \\ F_y &= -F (\sin(-\theta) + \mu \cos(-\theta)) . \end{aligned} \tag{12}$$

**a) First example problem**



**b) Second example problem**

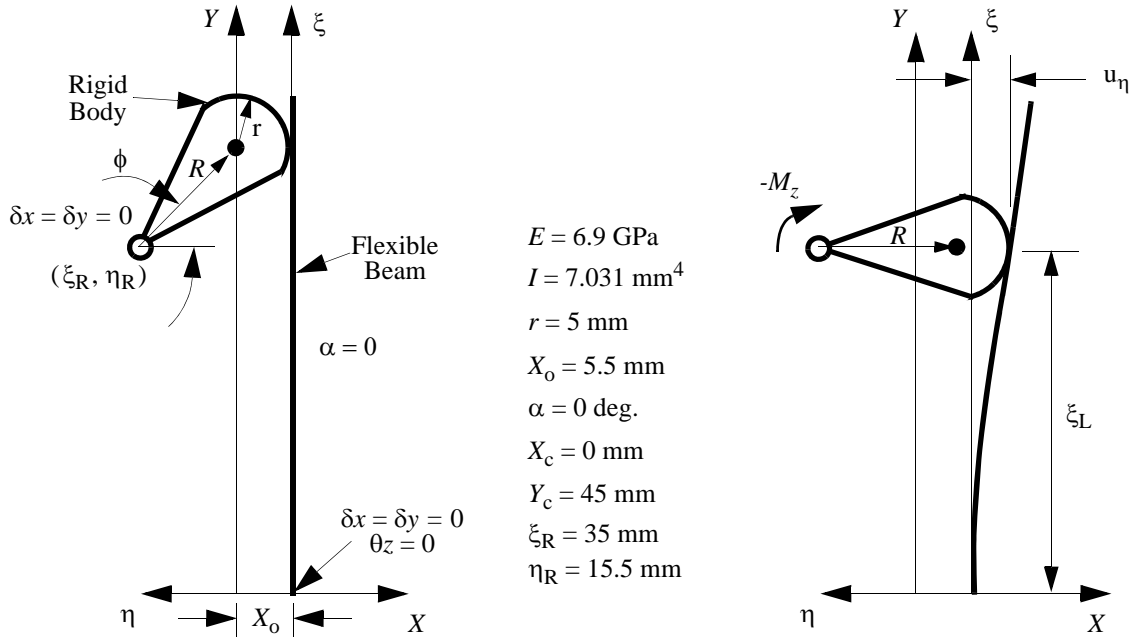
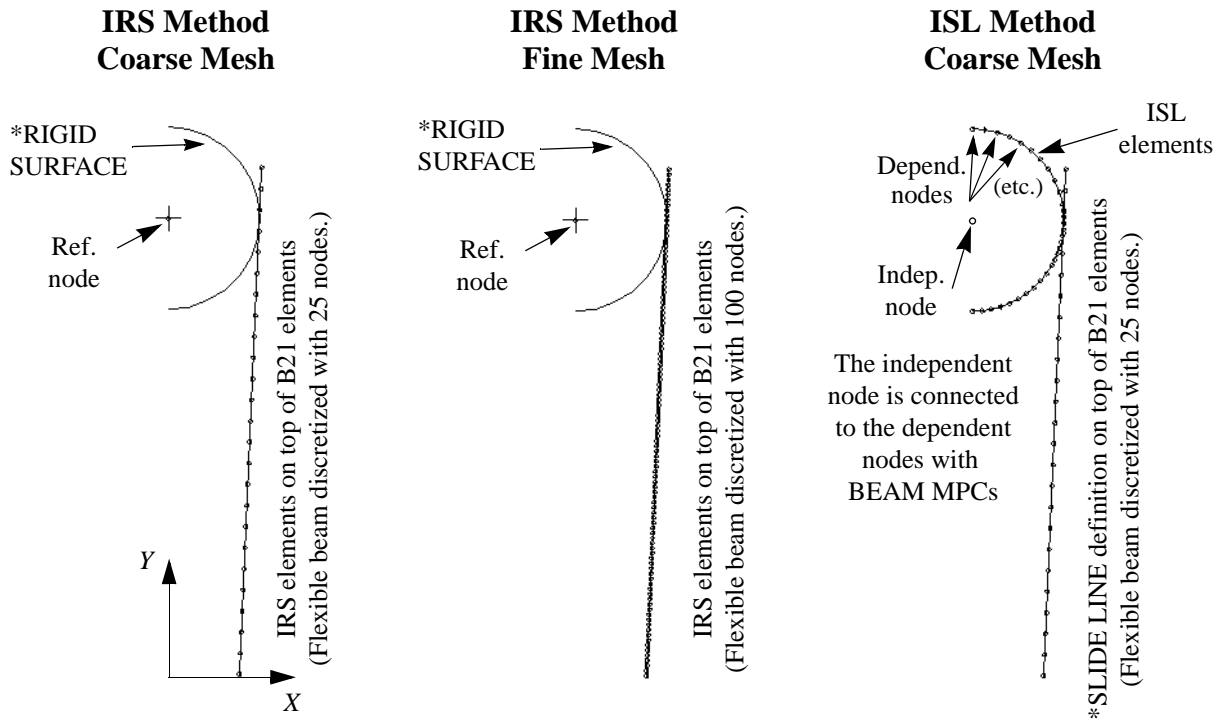


**Figure 1: Schematics of example problems to be studied.**



**Blow-up of contact region for all three models**

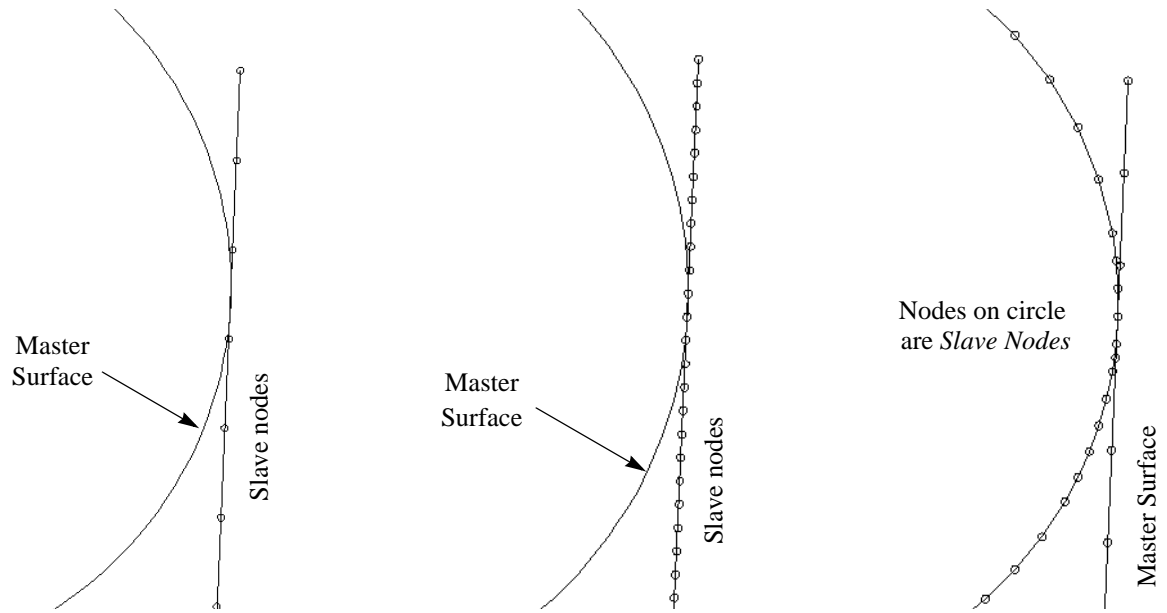


**Figure 2: Finite element models used to analyze first example problem.**

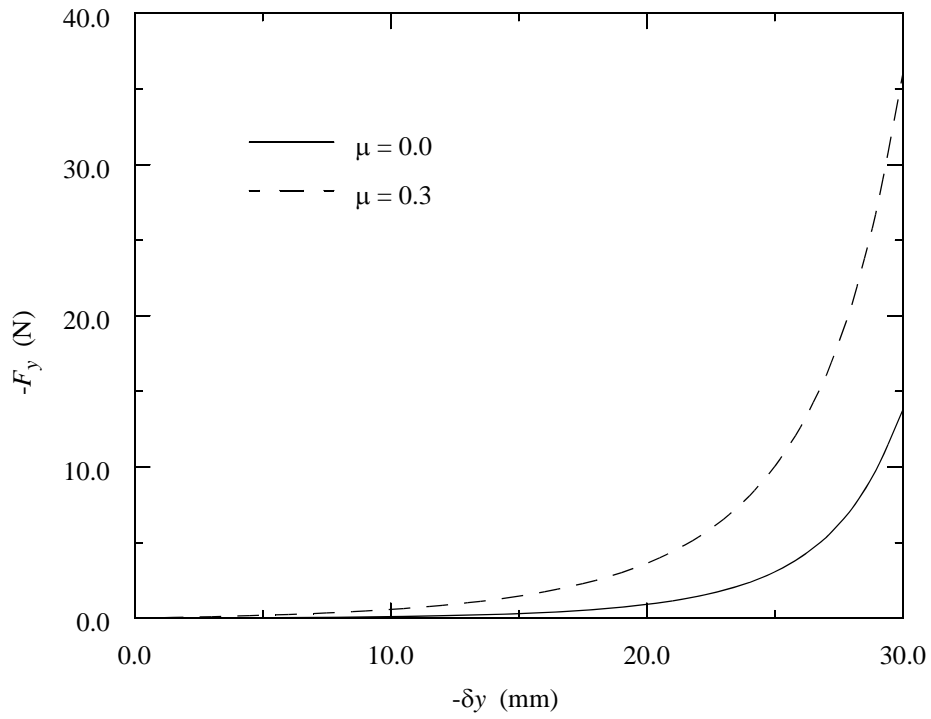


**Figure 3: Theoretical answer of first example problem with and without friction.**

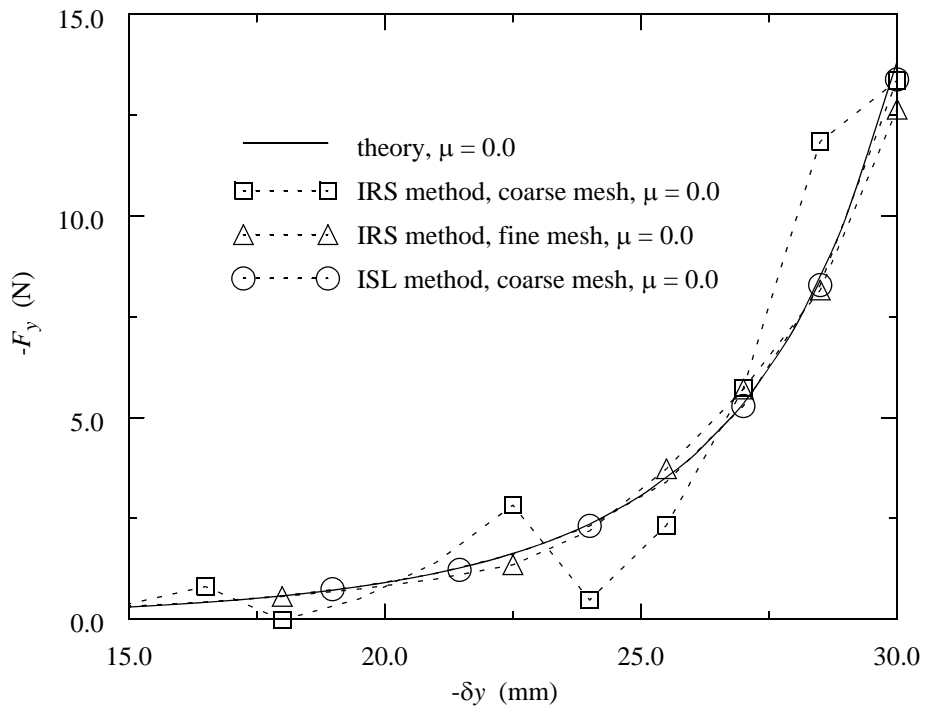
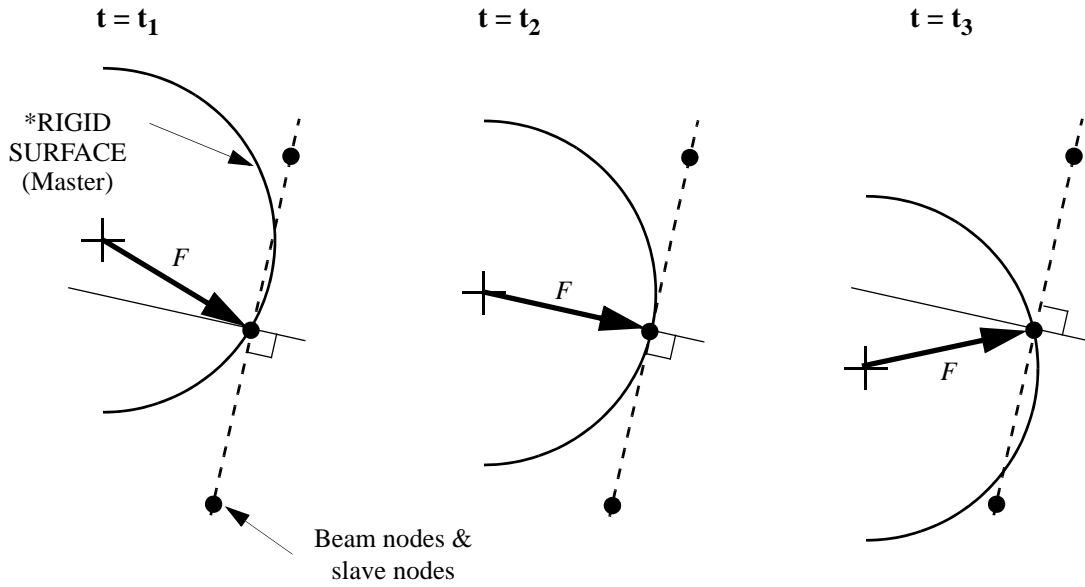
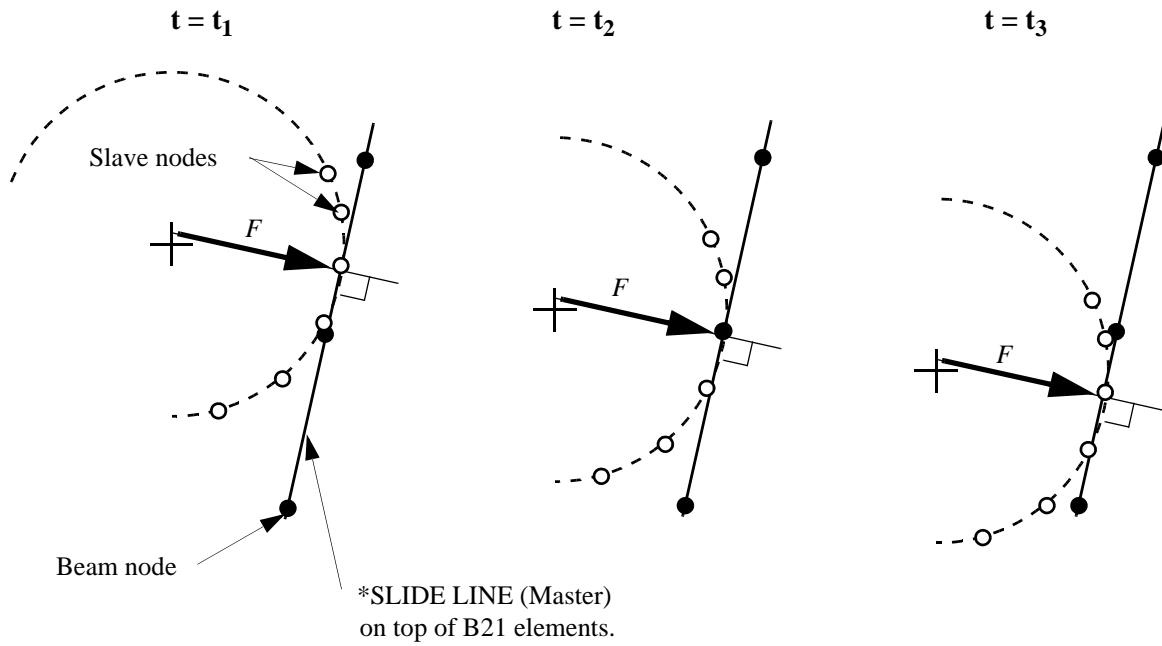


**Figure 4: Comparing different FE models of first example problem without friction.**

**a) IRS method**



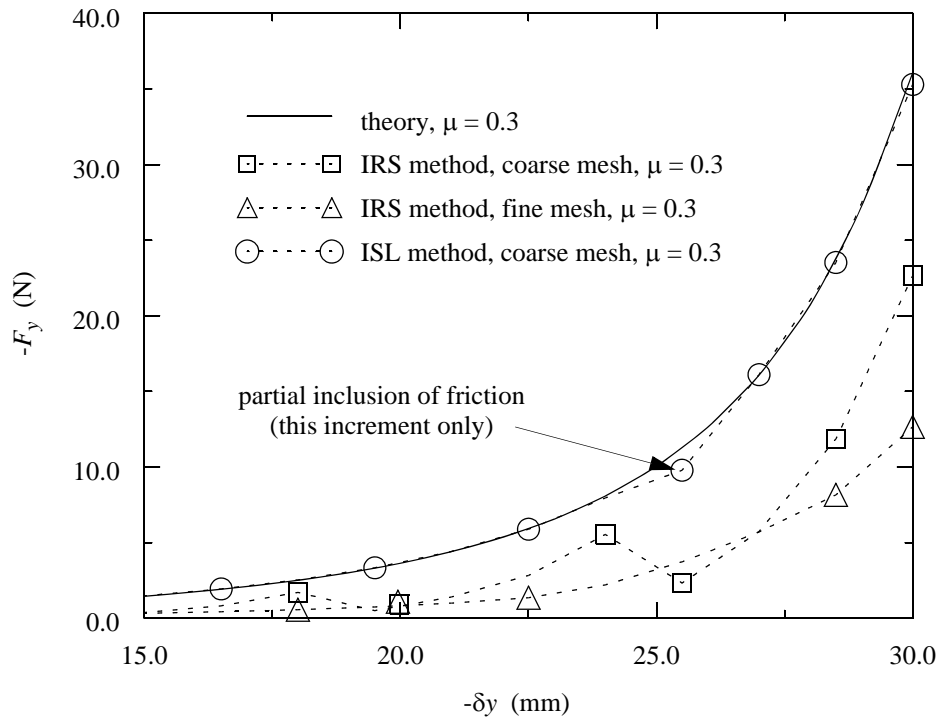
**b) ISL method**



Note: In a Master/Slave contact algorithm, the slave node is not allowed to penetrate the Master surface. Nothing prevents the Master surface from penetrating the surface between the slave nodes.

**Figure 5: Normal contact forces for IRS and ISL methods.**

**a) FE Results using current ABAQUS friction implementation**



**b) FE Results using *modified* friction implementation**

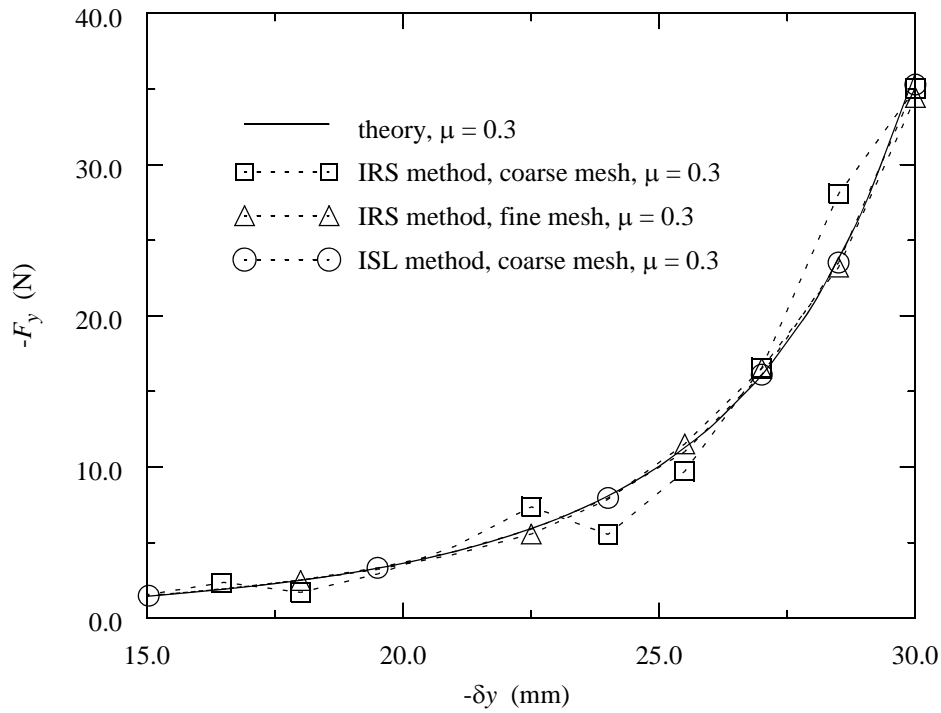


**Figure 6: Comparing different FE models of first example problem with friction.**

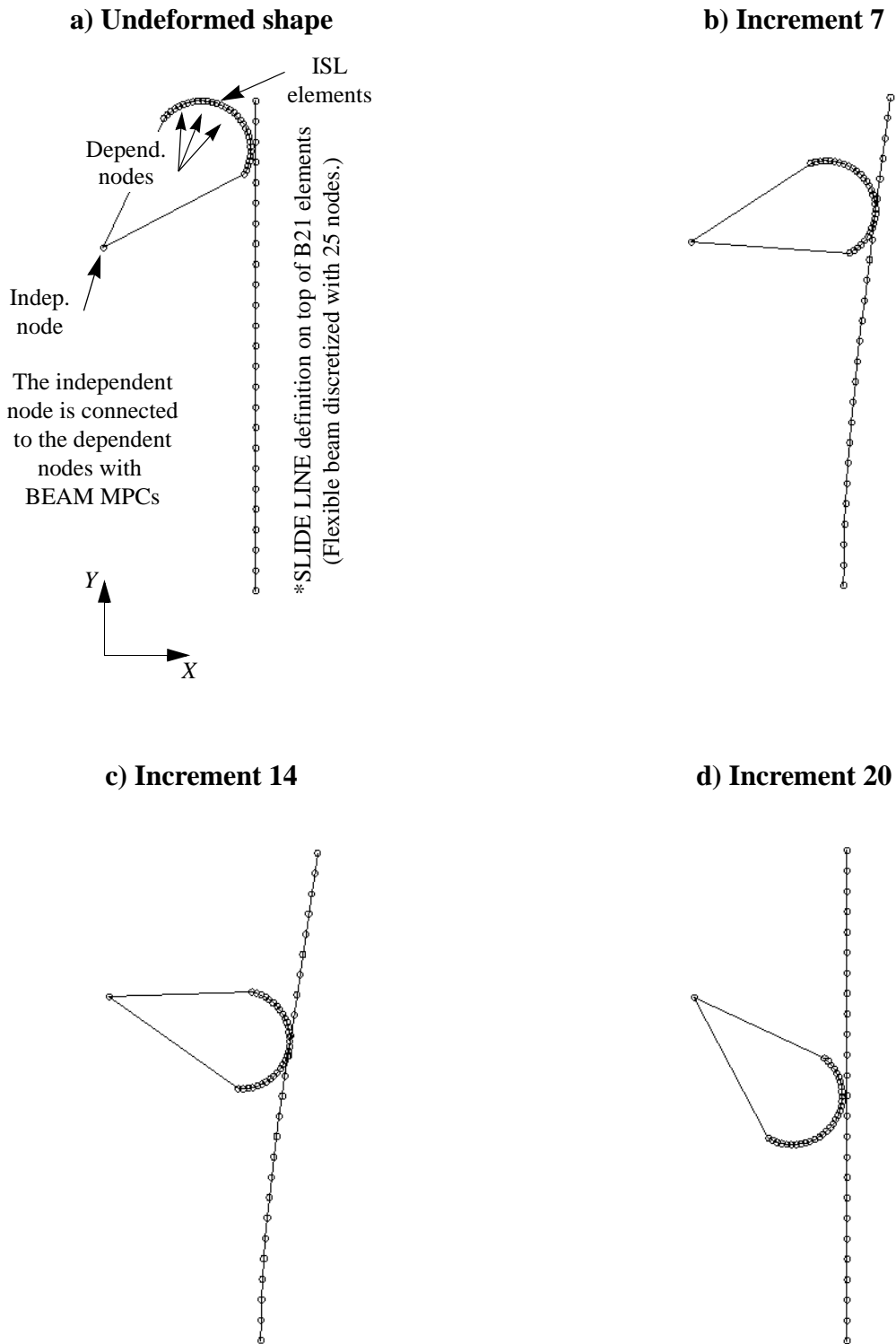


**Figure 7: ISL Model of second example problem: simulation of a rigid cam being rotated into a flexible member.**

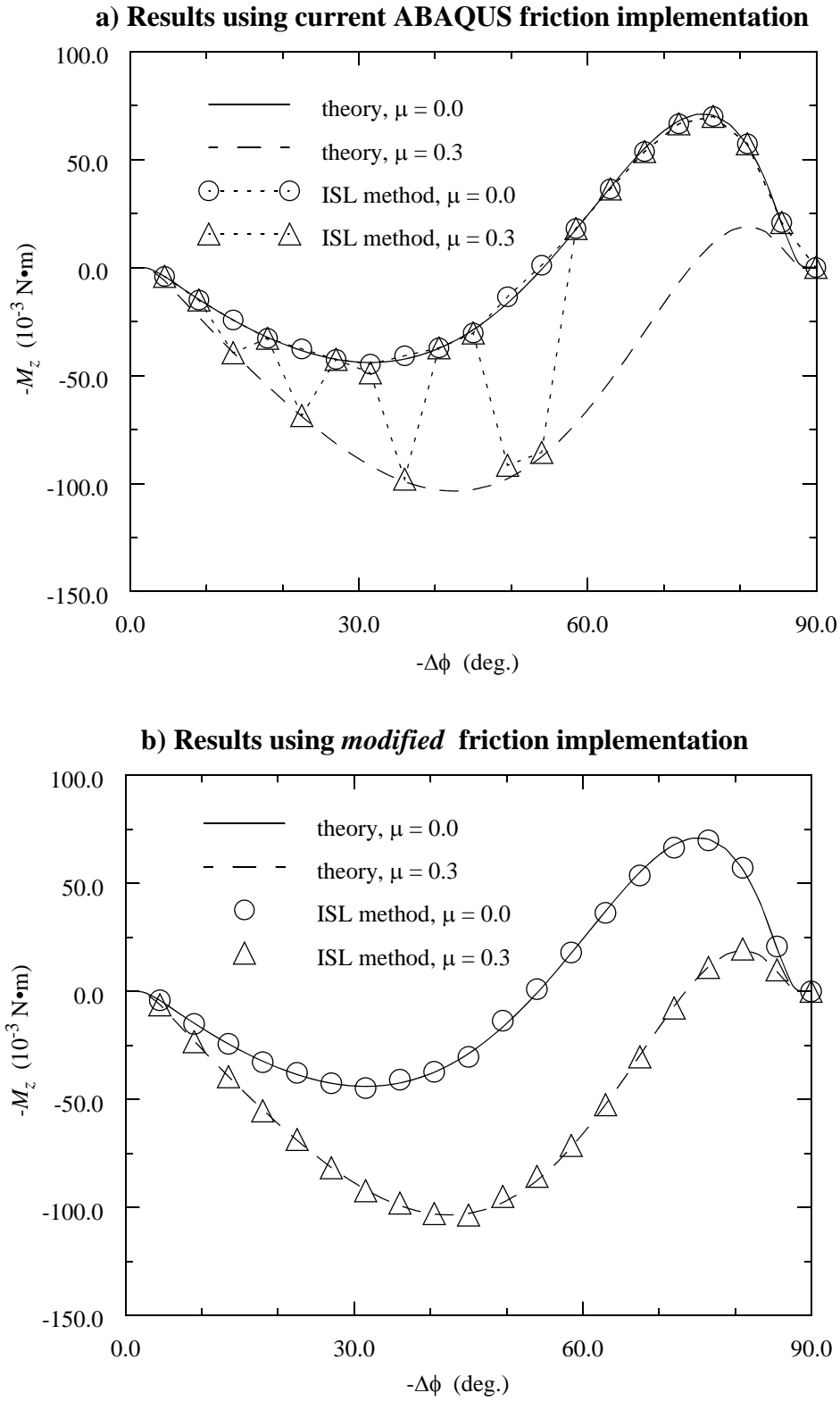


**Figure 8: Further demonstration of solution accuracy with modified friction implementation: second example problem.**

## IRS Method, Coarse Mesh, First Example, No Friction.

```
*HEADING
p1_irs_m1_mu00_soft.inp
*RESTART, WRITE, FREQ=1
** UNITS, LENGTH = m, Mass = kg, Time = sec, Force = N
*NODE, NSET=BEAM
1, 7.0E-3, 0.0
25, 9.222E-3, 50.0E-3, 0.0
*NGEN, NSET=BEAM
1,25,1
*ELEMENT, TYPE=B21, ELSET=BEAM
101, 1, 2
*ELGEN, ELSET=BEAM
101, 24, 1,1
*BEAM SECTION, ELSET=BEAM, SECTION=RECT, MATERIAL=POLYCARB, POISSON=0.3
25.0E-3,1.5E-3
*MATERIAL, NAME=POLYCARB
*ELASTIC,TYPE=ISO
6.9E9, 0.3
***** RIGID BEARING DEFINITION AND IRS ELEMENTS *****
*NODE, NSET=BEARINGC
9999, 0.0,45.0E-3, 0.0
*RIGID SURFACE, ELSET=IRS, TYPE=SEGMENTS
START, 0.0,54.0E-3
CIRCL, 9.0E-3,45.0E-3, 0.0,45.0E-3
CIRCL, 0.0,36.0E-3, 0.0,45.0E-3
*ELEMENT, TYPE=IRS21, ELSET=IRS
9901, 2, 3, 9999
*ELGEN, ELSET=IRS
9901, 23, 1,1
*INTERFACE, ELSET=IRS
25.0E-3
*FRICTION
0.0
*SURFACE CONTACT, SOFTENED
1.0E-5,4.8E6
*NSET,NSET=NOUT
BEARINGC,
**
*****
**
*STEP, NLGEOM, INC=100
MOVE BEARING DOWN
*STATIC
0.05, 1.0, 1.0E-6, 0.05
**
*BOUNDARY, TYPE=DISPLACEMENT, OPT=MOD
1, 1,6, 0.0
9999, 1,, 0.0
9999, 3,6, 0.0
9999, 2,, -30.0E-3
**
*CONTROLS, ANALYSIS=DISCONTINUOUS
*PRINT, CONTACT=YES
*END STEP
```

## ISL Method, Coarse Mesh, First Example, No Friction.

```
*HEADING
p1_isl_m1_mu00.inp
*RESTART, WRITE, FREQ=1
** UNITS, LENGTH = m, Mass = kg, Time = sec, Force = N
*NODE, NSET=BEAM
1, 7.0E-3, 0.0
25, 9.222E-3, 50.0E-3, 0.0
*NGEN, NSET=BEAM
1,25,1
*ELEMENT, TYPE=B21, ELSET=BEAM
101, 1, 2
*ELGEN, ELSET=BEAM
101, 24, 1,1
*BEAM SECTION, ELSET=BEAM, SECTION=RECT, MATERIAL=POLYCARB, POISSON=0.3
25.0E-3,1.5E-3
*MATERIAL, NAME=POLYCARB
*ELASTIC,TYPE=ISO
6.9E9, 0.3
***** RIGID BEARING DEFINITION AND SLIDE LINE *****
*NODE, NSET=BEARINGC
9999, 0.0,45.0E-3, 0.0
**
*NODE, NSET=BEARING
9000, 9.0E-3, 0.0
9010, 9.0E-3, 60.0
9020, 9.0E-3, 100.0
9030, 9.0E-3, 180.0
*NGEN,NSET=BEARING
9000,9010,1
9010,9020,1
9020,9030,1
*NMAP, NSET=BEARING, TYPE=CYLINDRICAL
0.0,45.0E-3,0.0, 0.0,45.0E-3,1.0
0.0,-1.0E-3,0.0
1.0,1.0,1.0
*MPC
BEAM, BEARING, 9999
**
** The following elements are for plotting purposes only
*ELEMENT, TYPE=B21, ELSET=DUMMY
9001, 9000, 9001
*ELGEN, ELSET=DUMMY
9001, 30, 1,1
*BEAM SECTION, ELSET=DUMMY, SECTION=RECT, MATERIAL=POLYCARB, POISSON=0.3
25.0E-3,1.5E-3
**
** DEFINE ISL & SLIDELINE
*ELEMENT, TYPE=ISL21, ELSET=ISL
9901, 9000, 9001
*ELGEN, ELSET=ISL
9901, 20, 1,1
** The SMOOTH parameter below should be set >0 and <0.5.
*SLIDE LINE, TYPE=LINEAR, ELSET=ISL, SMOOTH=0.25, GENERATE
2, 25, 1
Continued on next page
```

ISL Method, Coarse Mesh, First Example, No Friction (Continued)

```
**INTERFACE, ELSET=ISL
25.0E-3
*FRICTION
0.0
*SURFACE CONTACT, SOFTENED
1.0E-5,4.8E6
**
*****
*NSET,NSET=NOUT
BEARINGC,
*STEP, NLGEOM, INC=100
MOVE BEARING DOWN
*STATIC
0.05, 1.0, 1.0E-6, 0.05
**
*BOUNDARY, TYPE=DISPLACEMENT, OPT=MOD
1, 1,6, 0.0
9999, 1,, 0.0
9999, 3,6, 0.0
9999, 2,, -30.0E-3
**
*CONTROLS, ANALYSIS=DISCONTINUOUS
*PRINT, CONTACT=YES
*END STEP
```